Dedicated protection with signal overlap in elastic optical networks

# Dedicated Protection with Signal Overlap in Elastic Optical Networks (EON)

F. Cugini, M. Ruiz, T. Foggi, L. Velasco, N. Sambo, and P. Castoldi

*Abstract*— **In optical dedicated path protection (1+1), the same optical signal is transmitted along both working and backup paths. Thus, in 1+1 the transmission parameters need to be configured according to the most impaired path, e.g. the backup one. This implies that the working signal is typically served with higher than necessary Quality of Transmission (QoT) and it occupies larger than necessary spectrum resources, leading to inefficient network resource utilization.**

**In this study, we propose to apply the recently introduced signal overlap technique to improve network efficiency of optical dedicated path protection. The signal overlap technique enables uncorrelated optical signals to be superimposed along the same spectrum resources. It relies on a cancellation detection strategy also exploited in wireless communications and recently applied on coherent optical receivers. In particular, this study summarizes the key aspect and transmission performance of the overlap technique and discusses its implementation complexity. Then, two signal overlap schemes namely, *working signal overlap* and *working and backup signal overlap* are introduced for effective optical dedicated path protection. An integer linear programming (ILP) formulation based on the Routing, Modulation, and Spectrum Allocation (RMSA) problem and an efficient heuristic are then presented to effectively assess the performance of the proposed overlap-based 1+1 protection strategy under various topologies and traffic profiles. In the considered simulative scenarios (e.g., network diameters well below thousand kilometers), results show that the more efficient *working and backup signal overlap* scheme significantly improves the accepted load of dedicated protection requests.**

*Index Terms*— **EON, signal overlap, protection, 1+1, cancellation, RSA, RMSA, ILP.**

## I. Introduction

In elastic optical networks (EONs) efficient utilization of network resources is enabled by the flexi-grid technology and by advanced transmission techniques based on coherent detection strategies [1]–[4]. EONs successfully exploit effective low-density parity check (LDPC) and Forward Error Correction (FEC) solutions [5], [6] as well as complex modulation formats, including polarization multiplexed quadrature phase shift keying (PM-QPSK) or polarization multiplexed 16 quadrature amplitude modulation (PM-16QAM).

Traditionally, in EON, an optical signal is constrained to occupy a dedicated frequency range, called frequency slot, with no sharing of spectrum resources with other optical signals. Indeed, the frequency slot is currently defined as the frequency range allocated to a slot within the flexible grid and unavailable to other slots [7], [8].

Recently, a novel technique for EON, called *signal overlap*, has been introduced to overcome this constraint and enable the sharing of optical spectrum resources among different signals [9], [10]. In particular, this technique enables the overlap over the same spectrum resources of two independent optical signals, such as those generated by different, not synchronized, source nodes.

The technique does not require global time synchronization in the whole network and it does not exploit orthogonal codes as in Optical Code-Division Multiple-Access (O-CDMA) solutions. Also, it does not rely on MIMO processing, because it would entail a joint and synchronized signal transmission. Instead, it relies on cancellation techniques typically considered for wireless networks [11], now applied in the context of optical networks. More specifically, the proposed technique is practically elaborated upon the work in [12], [13], and based on advanced coding technology, successive interference cancellation strategies and proper configuration of optical transmission parameters.

The technique is less spectrally efficient and more complex to implement than increasing the constellation size with non-overlapping frequency slots. In particular, as discussed in this paper, the overlap technique requires additional processing capabilities with respect to currently available receiver solutions. However, it is important to consider that: (i) as occurred for wireless transmission techniques in the latest years, the evolution of processing capabilities will relax such limitations, so that the implementation of more advanced optical transmission techniques will be simplified and enabled; and (ii) the technique enables different use cases for flexible networking, like the protection scheme considered in this work, not achievable by non-overlapping signals with increased constellation size.

The feasibility of the technique has been demonstrated both theoretically [9] and experimentally [10] for single point-to-point connections. In this paper, the overlap technique is proposed and exploited in the context of optical dedicated path protection (1+1). In particular, two schemes are proposed.

In the first scheme, called *working signal overlap*, the overlap technique is applied to working paths only. Differently with respect to traditional protection schemes in EON [14], the larger than necessary Optical Signal to Noise Ratio (OSNR) typically available on the (shortest) working path is not wasted. Instead, such extra quality of transmission (QoT) can

Manuscript received June 28, 2017. This work was presented in part at OFC [1]

F. Cugini (email: filippo.cugini@cnit.it) and T. Foggi, are with CNIT, Italy.

M. Ruiz and L. Velasco are with Optical Communications Group (GCO), Universitat Politecnica de Catalunya (UPC), Barcelona, Spain.

N. Sambo and P. Castoldi are with Scuola Superiore Sant'Anna, Pisa, Italy.

be conveniently exploited to support the overlap with a (partially) co-routed working path of a different connection, with the aim of improving the overall network utilization.

However, this scheme imposes strict requirements on the backup paths of a pair of connections whose working paths are overlapped. Specifically, those backup paths need to be allocated to the same frequency slot than working paths and consequently, backup paths cannot share any hop, i.e. backup paths must be link-disjoint. This fact leads to the need of finding a free continuous and contiguous frequency slot in a large number of links, which greatly reduces expected spectrum exploitation in EON. An illustrative example of how slot assignment constraints reduce potentially efficient routing schemes can be found in [15] for the use case of serving multicast demands by means of light-trees.

To overcome this, we propose a second signal overlap scheme, called *working and backup signal overlap*, where both working and backup paths of a pair of demands can be overlapped, thus relaxing previous backup routing requirements.

This paper is a significantly extended version of the work reported in [1], where the transmission and networking performance of working signal overlap was presented for a preliminary scenario considering PM-QPSK. In particular, the novel contributions are:

- we extend the discussion on the applicability of the technique and on its implementation complexity for two signal overlap schemes namely, *i*) *working signal overlap*, and *ii*) *working and backup signal overlap*. A comprehensive introduction to signal overlap and our contributions to the 1+1 protection scenario are detailed in sections II and III;
- we define, for the first time, the *1+1 Protection with Signal Overlap Provisioning in EON* problem, hereafter referred as the PROSPECT problem. This optimization problem belongs to the category of network provisioning problems and, since it is stated and modelled in a generic way, it can be applied either for static offline demand planning or for dynamic connection request provisioning. An integer linear programming (ILP) formulation based on the that of the Routing, Modulation format, and Spectrum Allocation (RMSA) problem, as well as a heuristic algorithm based on the Biased Random-Key Genetic Algorithm (BRKGA) meta-heuristic are presented in section IV;
- we carefully analyze the performance of the proposed 1+1 protection strategy exploiting both signal overlap schemes, comparing various topologies, traffic profiles, and relevant network metrics. Moreover, we introduced a more realistic networking scenario including PM-16QAM over 37.5GHz. This reduces the advantages of the overlap technique with respect to scenarios where only PM-QPSK over 50GHz are considered (i.e., as in [1]). The details of such numerical results are provided in section V.

## II. Signal Overlap Technique

In this section, we first summarize the working principle of the overlap technique detailed in [9]. Then, we introduce specific considerations on the applicability of such technique. The overlap technique allows two independent optical signals $S_A$ and $S_B$ to be modulated and transmitted over the same optical spectrum resources and to be correctly received and detected.

Fig. 1 shows a schematic reference network scenario where the overlap technique is applied. Two PM-QPSK signals $S_A$ and $S_B$ are transmitted from node *A* and *B* towards node *D*, at the same central frequency $f_o$. To highlight the independency between the two optical signals (i.e., no orthogonal codes or synchronization are adopted), the scenario considers the two signals generated from two disjoint nodes.

The overlap technique exploits LDPC/FEC to guarantee adequate robustness. For example, when a gross rate of 112 Gb/s is considered, LDPC code rate *r* of 9/10 (9 bits of information out of 10 transmitted) provides remarkable robustness while guaranteeing net bit rate of around 100 Gb/s.

Moreover, the overlap technique exploits proper settings of the signal power levels. In particular, the power of $S_A$ is set at the superimposition point (i.e., node *B* in Fig. 1) to a higher value than the one of signal $S_B$. At node *B*, the two signals overlap. The two overlapped signals $S_A + S_B$ are then jointly propagated along *B*-*C*-*D* towards destination node *D*.

At the receiver, after the coherent opto-electronic conversion of the *overall* signal $S_A + S_B$, sampling and digital signal processing (DSP) are performed.

First, the detection is performed as if only $S_A$ were transmitted, i.e., considering $S_B$ simply as interference. This way, the coded signal $S_A$ is retrieved from the acquired data. Then, if detection of $S_B$ is needed, the acquired data are reprocessed to perform the cancellation of signal $S_A$. Once the cancellation is complete, a second detection stage is performed on the interfering coded channel $S_B$.

The technique was derived from the wireless technology (see [12] and references therein). The performance analysis exploits the auxiliary channel approach and the principle of mismatch detection (see [16], [17]). As computed in Sect. V, adequate OSNR performance is required to successfully detect both signals. Indeed, the re-modulation of $S_A$ may have limited accuracy, as some impairments are difficult to be estimated (e.g. nonlinear effects) and the detection of $S_B$ is also affected by the noise from the $S_A$ lightpath. We also remind to [9] for additional technical details on the overlap technique.

To be successfully adopted, the overlap technique requires a specific feature in intermediate nodes, and in particular within their bandwidth-variable wavelength selective switches (BV-WSSes). This BV-WSS feature enables, besides the traditional ability to direct different portions of the spectrum to different output ports, also the capability to perform power coupling over different ports, with adjustable attenuation capabilities. For example, with reference to Fig. 1, the new feature applies in the BV-WSS at the superimposition point (i.e., within node

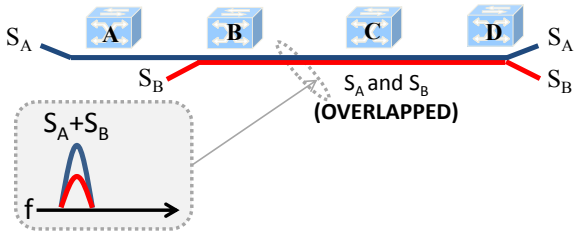


Fig. 1. Example of signal overlap applied on a reference network scenario.

*B*), to allow both ports receiving signals $S_A$ and $S_B$ to couple the frequencies around $f_0$ in the output port towards node *C*, with signal $S_B$ properly attenuated. Notice that this feature is already available in today's BV-WSS [18].

In the following we assess the processing capabilities required at the receiver to properly support the overlap technique.

As mentioned, the overlap technique is based on the cancellation of the first detected signal $S_A$. This operation clearly entails an increased processing at the receiver, and an additional latency for the detection of the underlying signal $S_B$. However, the computational burden is less remarkable than it could be expected, since it can be straightforwardly compared to equalization. As a matter of fact, the estimation of the required time-varying channel coefficients (see [9]) consists in the same operations as the equalization processing, at equal number of tap coefficients; it can be shown that re-modulation of the signal to be cancelled envisages $4L_{eq}$ complex multiplications per symbol, in the time domain, where $L_{eq}$ is the number of tap coefficients [19]. Clearly, as for equalization, these operations can be performed through fast Fourier transform (FFT), which turns out to be computationally more effective already for equalizer lengths of a few taps.

On the other hand, the complexity of the tap coefficients update depends on the time-varying rate of the channel, therefore the error function can be just updated at each symbol interval, whereas the coefficients update can be performed once every $N^{up}$ symbol intervals; hence, the complexity of this operation is highly variable, but, generally, much lower than equalization (or signal re-modulation) itself.

Then, the estimation of the signal phase entails a sliding window filtering which can be simply implemented recursively, thus implying just two complex multiplication per symbol (one to update the summation terms and one to obtain the re-modulated sample), and two additions (actually, a new term is added and the older one is subtracted)[1]. Therefore, if, for instance, we compare the complexity of the cancellation processing to the complexity of the iterative LDPC decoding (see [20]), it can be noticed that the computational increase is limited[2]. As concerns the latency, it is clearly required to detect a whole codeword of the signal $S_A$ in order to have availability of the symbols that must be re-modulated, whereas the re-modulation and cancellation operations can just advance the processing of signal $S_B$ of a few tens of symbols (depending on the number of channel taps and the width of the phase estimation sliding window). In order to clarify, TABLE 1 summarizes the computational load of the mentioned processing (equalization and channel identification are assumed to be performed in the frequency domain).

TABLE 1: COMPUTATIONAL LOAD COMPARISON (OPERATIONS PER SYMBOL) IN TERMS OF COMPLEX OPERATIONS. IN THE EXAMPLE, $N$=64800, $M$=6480, $u$=4, $t$=31, $q$=2 [20].

| | | Complex operations | Numerical examples |
|---|---|---|---|
| Equalization / Channel ident. | Mult: | Log($N$)+4 | ~15 |
| | Add: | 2 | 2 |
| Phase estimation | Mult: | 2 | 2 |
| | Add: | 2 | 2 |
| LDPC Decoding | Mult: | 0 | 0 |
| | Add: | $2\cdot(3\cdot u\text{-}4)\cdot M\cdot(q\text{-}1)^2 + u\cdot M\cdot(t\text{-}1)\cdot(q\text{-}1)$ | ~15 |
| | Max*: | $2\cdot(3\cdot u\text{-}4)\cdot M\cdot(q\text{-}1)^2$ | ~2 |

## III. SIGNAL OVERLAP FOR PROTECTION

### *A. Traditional 1+1 protection in EON*

Fig. 2 shows an enhanced version of the previous reference network scenario, where a traditional 1+1 protection solution is considered. No signal overlap is assumed in Fig. 2a. An optical signal $S_A$ is generated at source node *A* at central frequency $f_0$ and transmitted along the working path *A*-*B*-*C*-*D*. A second signal $S_B$ is added at node *B* at a different central frequency $f_1$ and transmitted along the working path *B*-*C*-*D*. The two signals coexist along the links *B*-*C* and *C*-*D*, occupying two different (i.e., non-overlapping) frequency slots on each of these links. Both signals are configured with 1+1 optical protection [14]. In particular, a replica of signal $S_A$ obtained with optical split at node *A* is transmitted along the protection path passing through node *G*. Similarly, signal $S_B$ is split at node *B* and transmitted along the protection path passing through node *F*. Traditionally, the working path is selected as the shortest one between source and destination, while its protection is selected as the shortest path being disjoint with the working one. The transmission parameters configured for each signal are then imposed by the most impaired path, i.e. the protection one. That is, on the working path the optical signal experiences higher than necessary QoT and typically occupies unnecessary spectrum resources. For example, if $S_A$ and $S_B$ in the working paths could be operated with PM-16QAM modulation format over 37.5 GHz, but their protection path require a more robust format like PM-QPSK over 50 GHz, given the optical protection, both working and protection of each of the two signals have to be operated with PM-QPSK over 50GHz. That is, additional 12.5GHz spectrum resources per signal have to be occupied along the working

[1]It is worth noting that the phase estimation performed during the detection processing can be also exploited to re-modulate the signal.

[2]We avoid to go into details concerning the complexity of each arithmetical operations since they are generally strictly related to specific hardware implementations.

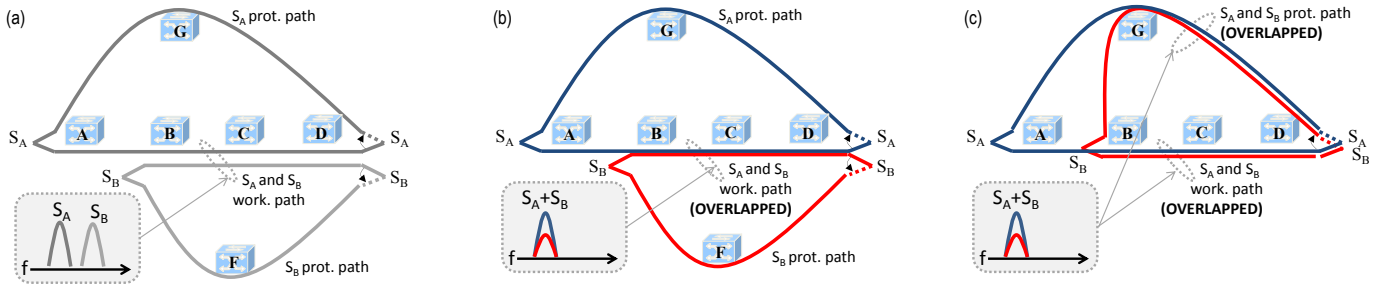


Fig. 2. 1+1 protection: (a) traditional approach with two working signals occupying different spectrum resources; (b) proposed "working signal overlap scheme" sharing spectrum resources on two different working signals; (c) proposed "working and backup signal overlap scheme" exploiting the overlap technique to share spectrum resources on both working and backup paths.

path, which reaches the destination with higher than necessary QoT. Overall, 100 GHz are occupied on the common links along the working path (e.g., links *B-C* and *C-D*).

### *B. Proposed 1+1 protection exploiting the overlap technique*

Two differentiated schemes have been proposed to apply the 1+1 overlap technique: *i*) *working signal overlap scheme* (Fig. 2b) and *ii*) *working and backup signal overlap scheme* (Fig. 2c). In these cases, both signals $S_A$ and $S_B$ are transmitted at the same central frequency $f_0$.

Fig. 2b shows the previously considered network scenario when the proposed 1+1 overlap technique is applied on working paths only. At node *B*, the two working signals $S_A$ and $S_B$, transmitted at the same central frequency $f_0$, overlap. It is important to highlight that node B can be placed anywhere over *A-D*. Indeed, the two signals (i.e., $S_A$ + $S_B$) can jointly propagate from any distance, subject that adequate QoT is guaranteed. To enable successful detection of either signal, the overlap technique is implemented taking advantage of the available extra QoT along the working paths.

Fig. 2c shows the proposed 1+1 overlap technique applied to both working and backup paths. As in the previous scheme, at node *B*, the two working signals $S_A$ and $S_B$ transmitted at $f_0$ overlap. In addition, here the two related backup signals overlap at node *G*. That is, in this scheme the two signals (i.e., $S_A + S_B$) jointly propagate along both *B-C-D* and *G-D*.

Both the aforementioned schemes can be considered according to the QoT of the considered signals. More specifically, if working signals support signal overlap while no adequate QoT is experienced by backup paths to exploit signal overlap, then the first working signal overlap scheme is exploited, enabling only working paths to be conveniently overlapped. Alternatively, if both working and protection signals have adequate QoT to support signal overlap, then the second working and backup signal overlap scheme is exploited, enabling both working and protection paths to be possibly overlapped.

When overlap is applicable, remarkable spectrum savings can be experienced. For example, with reference to the previous network scenario (i.e. the traditional one where $S_A$ and $S_B$ have to use PM-QPSK occupying 100 GHz on common working links while experiencing extra QoT), the proposed 1+1 technique provides significant benefits. Indeed, such extra QoT is exploited to enable the proposed overlap of the two signals, occupying a total amount of just 50 GHz along the working path (e.g., 50GHz along B-C and C-D in Fig. 2). Moreover, if adequate QoT is available also on the backup paths, additional spectrum savings can be experienced also along the protection resources (e.g., 50GHz along G-D in Fig. 2).

## IV. The PROSPECT Problem

### *A. Problem statement*

The PROSPECT problem can be formally stated as follows:

Given:

- an EON, represented by a directed connected graph $G(V, E)$, being $V$ the set of optical nodes and $E$ the set of fiber links connecting two nodes in $V$;
- an ordered set $S$ of frequency slices in each link in $E$; $S = \{s_1, s_2, ..., s_{|S|}\}$;
- the set of modulation formats $M$. Each modulation format $m$ is represented by the tuple $<f_m, r_m, h_m>$, where $f_m$ is the spectral efficiency, $r_m$ is the optical reach, and $h_m$ the maximum signal overlap distance (note that $h_m \leq r_m$);
- a set $D$ of demands to be transported. Each demand $d$ is represented by a tuple $<o_d, t_d, b_d>$, where $o_d, t_d \in V$ are the source and the destination nodes respectively, and $b_d$ is the requested bitrate;
- the signal overlap scheme, including no overlap, only working signal overlap or working and backup signal overlap.

Output: the route, modulation format and spectrum allocation of two link-disjoint optical connections for every served demand $d \in D$, allowing signal overlap according the selected scheme between pair of demands.

Objective: minimize the amount of rejected demands (primary objective) and the total amount of used spectrum slices (secondary objective).

### *B. Mathematical model*

The formulation of the PROSPECT problem is based on that of the basic RMSA problem presented in [21]. We have conveniently extended such basic formulation to consider 1+1 protection and signal overlap. Among those different alternatives in [21], we selected the link-path formulation that requires precomputing, for every demand $d$, a set of allowable

routes $P(d)$ and a set of spectrum slots $C(d)$. Each slot consists in a given modulation format and a set of contiguous spectrum slices that allow serving the bitrate of the demand according to the spectral efficiency of the selected modulation format.

It is worth noting that the major complexity of the PROSPECT problems resides in guaranteeing feasible signal overlap among demands. Inspired on the concept of the abovementioned path and slot sets pre-computation, we define the signal overlap tuples set $Q$ that stores all candidate signal overlap between pairs of demands that might be selected during optimization.

Table II shows the pseudocode for pre-computing set $Q$. After initializing $Q$ to the empty set, all distinct pairs of demands that share the destination node are evaluated (lines 1-3 in Table II). Then, every allowable slot common for both demands is selected, provided that the associated modulation format allows signal overlap i.e., the maximum overlap distance is greater than 0 (lines 4-6). Once a demand pair $\{d_i, d_j\}$ and a slot $c$ has been selected, every combination of working paths $\{p_i, p_j\}$ and backup paths $\{b_i, b_j\}$ is checked, provided that all paths accomplish the optical reach of the modulation format (lines 7-11).

At this point, the set of common hops shared from any intermediate node to destination is retrieved for working paths and backup paths (lines 12 and 13). Note that if only working overlap signal is allowed, no backup signal overlap is considered, as well as overlap is not possible if there is no link sharing among paths (lines 14-15). On the other hand, signal overlap of working paths and/or backup paths is allowable if and only if paths length remain lower or equal than the maximum signal overlap distance (lines 16-17). The obtained signal overlap tuple, that is stored in $Q$, contains the pair of demands, working paths, backup paths, and slot (line 18). The set $Q$ is eventually returned after the exhaustive exploration of sets $D$, $P$, and $C$ (line 19).

TABLE II SET $Q$ PRE-COMPUTATION

```
INPUT D,P,C, scheme
OUTPUT Q
1:    Q←Ø
2:    for {di,dj}∈D²|di≠dj do
3:      if di.t≠dj.t then continue
4:      for c∈C(di)⋂C(dj) do
5:        h←getSignalOverlapDist(c.m)
6:        if h==0 then continue
7:        r←getReach(c.m)
8:        for {pi,bi}∈P²(di)|E(pi)⋂E(bi)=Ø do
9:          if max(l(pi),l(bi))>r then continue
10:         for {pj,bj}∈P²(dj)|E(pj)⋂E(bj)=Ø do
11:           if max(l(pj),l(bj))>r then continue
12:           Ep←commonHopsToDest(pi,pj)
13:           Eb←commonHopsToDest(bi,bj)
14:           if scheme=='working' and Eb≠Ø then
              continue
15:           if Ep=Ø and Eb=Ø then continue
16:           if Ep≠Ø and max(l(pi),l(pj))>h then
              continue
17:           if Eb≠Ø and max(l(bi),l(bj))>h then
              continue
18:           Q←Q∪<di,dj,pi,pj,bi,bj,c,Ep,Eb>
19:   return Q
```

Before detailing the mathematical formulation of the problem, the following sets and parameters need to be defined:

| | |
|---|---|
| $V$ | Set of optical nodes, index $v$. |
| $E$ | Set of optical links, index $e$. |
| $D$ | Set of demands, index $d$. |
| $s_d$, $t_d$ | Source and destination nodes of demand $d$ |
| $b_d$ | Bitrate (in Gb/s) of demand $d$ |
| $M$ | Set of modulation formats, index $m$ |
| $f_m$ | Spectral efficiency (in b/s/Hz) of modulation format $m$ |
| $r_m$ | Optical reach (in km) of modulation format $m$ |
| $h_m$ | Maximum overlap distance (in km) of modulation format $m$ |
| $S$ | Set of frequency slices, index $s$. |
| $\delta_{es}$ | Equal to 1 if slice $s$ is free in link $e$; 0 otherwise. |
| $C$ | Set of frequency slots, index $c$ |
| $C(d)$ | Subset of C with slots for demand $d$ |
| $\delta_{cm}$ | Equal to 1 if slot $c$ has assigned modulation format $m$; 0 otherwise. |
| $\delta_{cs}$ | Equal to 1 if slot $c$ contains slice $s$; 0 otherwise. |
| $P$ | Set of optical routes, index $p$. |
| $P(d)$ | Subset of P with routes for demand $d$. |
| $\delta_{pe}$ | Equal to 1 if path $p$ uses link $e$; 0 otherwise. |
| $l_p$ | Length in km of path $p$ |
| $Q$ | Set of pre-computed signal overlap tuples, index $q$ |
| $Q(d)$ | Subset of $Q$ for demand $d$ |
| $\pi_{qpc}$ | Equal to 1 if tuple $q$ contains working path $p$ and slot $c$; 0 otherwise. |
| $\rho_{qpc}$ | Equal to 1 if tuple $q$ contains backup path $p$ and slot $c$; 0 otherwise. |
| $\gamma_{qde}$ | Equal to 1 if demand $d$ does not account for capacity in link $E$ of tuple $q$; 0 otherwise. |
| $\alpha$ | Cost function multiplier. |

Note that binary parameters $\pi_{qpc}$, $\rho_{qpc}$, and $\gamma_{qde}$ are obtained from pre-processing tuples in $Q$. To guarantee correct slice usage accounting if tuple $q$ is selected, $\gamma_{qde}$ is equal to zero for all the links that are not part of the signal overlapping. On the contrary, $\gamma_{qde}$ is equal to 1 for those links in the signal overlapping of only one of the overlapped demands (being always zero for the other).

In addition to the previous notation for sets and parameters, the following decision variables are required:

| | |
|---|---|
| $x_{pc}$ | Binary, equal to 1 if path $p$ and slot $c$ are selected for working routing; 0, otherwise. |
| $y_{pc}$ | Binary, equal to 1 if path $p$ and slot $c$ are selected for backup routing; 0, otherwise. |
| $u_d$ | Binary, equal to 1 if demand $d$ is rejected; 0, otherwise. |

$w_{es}$ Binary, equal to 1 if slice $s$ in link $e$ is used; 0, otherwise.

$z_q$ Binary, equal to one if signal overlapping tuple $q$ is selected; 0, otherwise.

The ILP model for the PROSPECT problem is as follows:

$$Minimize \quad \alpha \cdot \sum_{d \in D} u_d + \sum_{e \in E} \sum_{s \in S} w_{es} \tag{1}$$

subject to:

$$\sum_{p \in P(d)} \sum_{c \in C(d)} x_{pc} + u_d = 1 \quad \forall d \in D \tag{2}$$

$$\sum_{p \in P(d)} \sum_{c \in C(d)} y_{pc} + u_d = 1 \quad \forall d \in D \tag{3}$$

$$\sum_{p \in P(d)} x_{pc} = \sum_{p \in P(d)} y_{pc} \quad \forall d \in D, c \in C(d) \tag{4}$$

$$\sum_{p \in P(d)} \sum_{c \in C(d)} \delta_{cm} \cdot l_p \cdot x_{pc} \le r_m \quad \forall d \in D, m \in M \tag{5}$$

$$\sum_{p \in P(d)} \sum_{c \in C(d)} \delta_{cm} \cdot l_p \cdot y_{pc} \le r_m \quad \forall d \in D, m \in M \tag{6}$$

$$\sum_{p \in P(d)} \delta_{pe} \cdot \sum_{c \in C(d)} (x_{pc} + y_{pc}) \le 1 \quad \forall d \in D, e \in E \tag{7}$$

$$\sum_{q \in Q(d)} z_q \le 1 \quad \forall d \in D \tag{8}$$

$$x_{pc} \ge \pi_{qpc} \cdot z_q \quad \forall d \in D, q \in Q(d), p \in P(d), c \in C(d) \tag{9}$$

$$y_{pc} \ge \rho_{qpc} \cdot z_q \quad \forall d \in D, q \in Q(d), p \in P(d), c \in C(d) \tag{10}$$

$$\sum_{d \in D} \sum_{p \in P(d)} \sum_{c \in C(d)} \delta_{pe} \cdot \delta_{cs} \cdot (x_{pc} + y_{pc} - \sum_{q \in Q(d)} \gamma_{qde} \cdot (\pi_{qpc} + \rho_{qpc}) z_q) \le \delta_{es} \cdot w_{es} \quad \forall e \in E, s \in S \tag{11}$$

The objective function (1) minimizes the amount of rejected demands and the total amount of used spectrum slices. Aiming at guaranteeing the desired objective function priority, $\alpha$ needs to be set to a large value, e.g. $|E| \cdot |S|$.

Constraints (2)-(7) deal with the RMSA of demands guaranteeing 1+1 protection. Constraint (2) guarantees that either a working path and slot is selected for a demand or the demand is rejected, whereas constraint (3) makes sure of an equivalent condition for the backup path. Constraint (4) forces the selection of the same slot for the working and backup path of a served demand. Constraints (5) and (6) guarantee that the length of the working and backup paths, respectively, do not exceeds the reach of the selected modulation format. Note that this condition is not guaranteed in pre-computation phase since paths and slots are pre-computed separately. Constraint (7) deals with link-disjointness of working and backup paths, by guaranteeing that every link can be part of the route of at most one of the paths.

Constraints (8)-(11) deal with signal overlap. Specifically, constraint (8) ensures that every single demand can be selected in at most one signal overlap. Constraint (9) forces to choose the working path specified in the selected signal overlap tuple. Note that constraint (10) is equivalent to constraint (9) for the backup path. Finally, constraint (11) computes slice occupancy taking into account the selected overlap tuples. Thus, two signals overlapped in the same slice of the same link account just once for the slice usage, being the capacity contribution of one of the demands cancelled, i.e. $\gamma_{qde}$=1.

The size of the PROSPECT problem formulation is O(|P|·|C|+|E|·|S|+|Q|) binary variables and O(|D|·|Q|·|P|·|C|+|E|·|S|) constraints. This translates into instances with $10^6$ variables and $10^{10}$ constraints for the national network scenarios considered in Section V. In view of this large size that makes unaffordable the exact resolution of the ILP model for realistic scenarios, in the following section we propose a heuristic algorithm to efficiently solve PROSPECT.

### C. Heuristic Algorithm

In this section, we propose a heuristic algorithm based on the BRKGA metaheuristic, a class of genetic algorithm that has been proposed to effectively solve EON-related optimization problems [21]. In this meta-heuristic, a set of individuals, called a population, evolves over a number of generations. Each individual solution is represented by an array of n genes named chromosome (*chr*), where each gene can take any value in the real interval [0,1]. Each *chr* encodes a solution of the problem and a fitness value i.e., the value of the objective function. The chromosome internal structure and the decoder algorithm that transforms chromosomes into solutions are detailed next.

The decoder (TABLE III) receives a chromosome that contains as genes as demands in $D$. Each gene encodes the order in which the demand related with such gene will be processed next. After some initializations, this chromosome is used to sort the set of demands according to the values of the genes in the chromosome (lines 1-2 of TABLE III). Then, following that order, a procedure transforms the ordered demands set $D$ into the ordered demand pairs set $\Phi$ and the ordered demand set $D_{rem}$ containing those unpaired demands (line 3). Pairs contain demands that share, at least, the destination node, although the sharing of both source and destination is preferred when overlapping in working and

TABLE III DECODER ALGORITHM

```
INPUT G,D,chr,type
OUTPUT sol,fitness
1:   fitness←0; sol←∅
2:   sort(D,chr)
3:   <Φ,D_rem>←groupInPairs(D,type)
4:   for <d_i,d_j>∈Φ do
5:     ite←RMSA_1+1_overlap(G,d_i,d_j,type)
6:     allocate(G,ite)
7:     sol←sol∪ite
8:   for d∈D_rem do
9:     ite←RMSA_1+1(G,d)
10:    allocate(G,ite)
11:    sol←sol∪ite
12:  fitness←evaluateFitness(sol)
13:  return sol,fitness
```

backup paths is allowed. The rationale behind this demand grouping is to increase the success in the search of potential signal overlap, since demands in a pair are processed together, as will be following detailed.

Each of the demand pairs in $\Phi$ is processed in order to find the RMSA for working and backup paths ensuring 1+1 protection and signal overlap (lines 4-5). Before processing the next pair, spectrum resources required by the current pair are allocated and the solution is updated (lines 6-7). Once all pairs have been processed, single demands in $D_{rem}$ are routed following a similar approach than that of routing demand pairs but considering no signal overlap (lines 8-12). Finally, fitness is evaluated and the solution returned (lines 12-13).

The details of the RMSA algorithm in line 5 are presented in Table IV. The algorithm receives the network $G$, the pair of demands $<d_i,d_j>$, and the considered signal overlap schemeand returns a solution that contains the route of working and backup paths (if feasible) of both demands and the slot including the modulation format. After some initializations, a set of $k$ pairs of link-disjoint routes for demand $d_i$ are computed (lines 1-2 of TABLE IV). Each of these link-disjoint route pairs is evaluated as working and backup paths of demand $d_i$ provided that a free slot exists, which is retrieved after analyzing current spectrum availability (lines 3-5). After this, a subgraph containing all the links where the selected slot is available is created to be next used to route demand $d_j$ (line 7). Note that this subgraph also contains the links present in selected working and backup paths of demand $d_i$ since they can be potentially reused for $d_j$ by means of signal overlap.

TABLE IV RMSA_1+1_OVERLAP

```
INPUT G,d_i,d_j,type
OUTPUT sol
1:    cost←∞; sol←Ø
2:    Ω←K-disjointPaths(G,d_i,k)
3:    for <p_i,b_i>∈Ω do
4:      slot←findSlot(G, p_i, b_i)
5:      if slot==Ø then continue
6:      h←slot.m.h
7:      G'←subGraph(G, slot)
8:      p_j←Ø
9:      for n in 0..|p_i|-2 do
10:       v=p_i[n];maxdist=h-l(p_i[n..|p_i|])
11:       p'_j←SP(G',d_j.s,v,maxdist)
12:       if p'_j==Ø then continue
13:       p_j←conc(p'_j,p_i[n+1,|p_i|])
14:       updateSubGraph(G',p_j,type)
15:       if type=='working' then
16:         maxdist=h
17:         b_j←SP(G',d_j.s,d_j.t, maxdist)
18:         if b_j==Ø then continue
19:       else
20:         auxcost←∞; b_j←Ø
21:         for m in 0..|b_i|-2 do
22:           u=b_i[m]
23:           maxdist=h-l(b_i[m..|b_i|])
24:           b'_j←SP(G',d_j.s,u,maxdist)
25:           if b'_j==Ø then continue
26:           b_jAux←conc(b'_j,b_i[m+1,|b_i|])
27:           c←evalCost(p_i,b_i,p_j,b_j,slot)
28:           if auxcost>c then
29:             auxcost←c
30:             b_j←b_jAux
31:         if b_j==Ø then continue
32:       c←evalCost(p_i,b_i,p_j,b_j,slot)
33:       if cost>c then
34:         cost←c
35:         sol←<p_i,b_i,p_j,b_j,slot>
36:   return sol
```

Aiming at exploiting signal overlap benefits, the procedure to find working and backup paths for $d_j$ is different from that used for demand $d_i$. Specifically, a sub-path from the source node of $d_j$ to any intermediate node in working path of $d_i$ is computed to construct a candidate working path for $d_j$ (lines 8-13). In case of finding a feasible candidate working path for $d_j$, (i.e. accomplishing maximum overlap distance $h$), two alternatives can be chosen for finding a candidate backup path for $d_j$. In case that signal overlap only applies to working paths, the subgraph is updated to avoid backup overlapping and only one shortest path from source to destination is computed (lines 14-18). On the contrary, a similar procedure than that used to find the best overlap for working signal is applied to the backup signal (lines 20-31). After evaluating every possible link disjoint routes pair for demand $d_i$ and overlapping paths for demand $d_j$, the one with the minimum cost in terms of the objective function is selected and eventually returned (lines 32-36).

The performance of the heuristic in terms of quality of the solution and execution time compared to that of the ILP model is analyzed in numerical results section.

## V. NUMERICAL RESULTS

### A. Transmission performance

The performance of the proposed 1+1 protection scheme enabled by the overlap technique is evaluated considering both transmission and networking performance. To assess the transmission performance, two independent PM-QPSK signals $S_A$ and $S_B$ are first considered at gross bit rate 112 Gb/s. The overlap technique is here applied targeting a net rate of 100 Gb/s for signal $S_A$ ($r_A$ = 9/10). Analog to digital converter (ADC) with analog bandwidth of 20 GHz and a sampling rate of 56 GSample/s is assumed. Both signals are filtered at transmitter and receiver side with 4th-order Gaussian optical filters with 35-GHz bandpass bandwidth, in-line with the traditional optical network requirements. The performance of the overlap technique has been evaluated by configuring code rates and power levels.

Fig. 3 shows the performance of the theoretical achievable bounds (AB) of the overlap technique. Results show that the limiting optical reach is imposed by $S_B$ (the 100 Gb/s scenario is verified on the left region of the $S_B$ curve). Moreover, the figure highlights the specific case at 100 Gb/s when a 3-dB margin is applied on theoretical bounds [9]. Results show that up to 800 km (on the 3-dB margin) can be successfully traversed by both overlapped signals with practical LDPC codes ($r_A$ = 9/10, $r_B$ = 9/10, $S_A$ / $S_B$ = 5.5dB). For the sake of

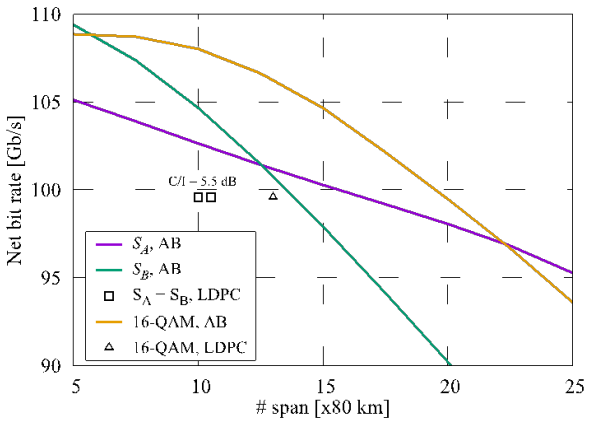


Fig. 3. Transmission performance of the overlap technique.

completeness, also the PM-16QAM performance is reported. The figure also highlights the specific case at 100 Gb/s when 3-dB margin is applied on the PM-16QAM theoretical bounds, showing that up to around 1000 km can be achieved by a PM 16QAM signal. Further details on the models and simulative scenarios and can be found in [9].

In view of these results, hereafter we assume that optical connections can be modulated using either 16-QAM (37.5GHz slot) or QPSK (50GHz slot). Optical reach is limited to 1000 km and 2500 km for 16-QAM and QPSK, respectively. Signal overlapping is permitted only with QPSK provided that the length of each overlapped signal never exceeds 800 km.

### *B. Network performance evaluation*

For evaluation purposes, we used two real topologies: the 14-node Deustche Telekom (DT) and the 30-node Telefonica (TEL) national networks (embedded in Fig. 4). Nodes can be classified into three subsets: nodes that are source/destination of traffic (black circles), gateway nodes (black squares), and transit nodes (white circles). The maximum shortest distance between any pair of source/destination nodes, which in our context represents the actual network diameter, is 725 km and 950 km for DT and TEL, respectively. A total spectrum width of 2THz divided into 12.5 GHz frequency slices is considered for all fiber links (in line with [22]).

An instance is defined by a network topology and a number of 100 Gb/s demands randomly generated according to one of the following distributions: *i*) both end nodes are randomly chosen among all traffic source/destination nodes, or *ii*) destination node is one of the gateway nodes. A traffic profile is defined as a mix of both distributions. Three traffic profiles characterized by the percentage of traffic targeting gateway nodes were used: TP-1 (5%), TP-2 (25%), and TP-3 (50%).

We implemented the ILP and the heuristic in Python, using CPLEX 12.5.1 as solver engine for the former. A set of small-size instances for DT topology were generated and solved with both methods with the sake of a comparative analysis in terms of quality of the obtained solutions and execution time. Using an Intel(R) Core(TM) i7-4790K CPU @ 4.00GHz machine with 4GB RAM running UBUNTU server 14.04.4 LTS and limiting ILP execution time to 10 hours, we solved to optimality a set of 100 instances. After solving such instances with the heuristic, we obtained a maximum optimality gap between heuristic solution and optimal solution as small as 5%, due to equal blocking performance but a lesser efficient use of spectrum resources of the heuristic compared with the ILP. Note that the largest instances requiring almost 10 hours of ILP computation time were solved by the heuristic in the order of only few seconds. Therefore, we validate the heuristic as an affordable method to provide good-quality solutions for the PROSPECT problem and hereafter, we use this method for comparative purposes of the proposed signal overlap schemes.

Numerical analysis of network performance in terms of blocking probability as a function of the normalized network load for every topology, traffic profile and signal overlap scheme is provided in Fig. 4. The very first evidence is that overlapping only working paths provides small, even negligible network performance gain. As anticipated in previous sections, a pair of demands using this signal overlap scheme require, in addition to sharing the same slot for both working and backup paths, routing backup paths through link-disjoint routes between them. Since almost every demand can be modulated as 16-QAM due to short path distances, the balance between those added spectrum resources caused by the need of modulating signals with QPSK and those saved resources caused by signal overlapping is frequently negative. Therefore, it is better to route demands using 16-QAM without overlapping. Moreover, even in the case where working overlap requires less overall spectrum resources than no overlap, such resources need to be available in the same slot for a large number of links i.e., working and backup paths of both demands. This fact makes more difficult to find free spectrum allocation and, consequently, reduces expected network performance gains.

Nevertheless, when overlap can be applied to both working and backup paths, high spectrum savings lead to significant load gains for DT (10-15%) and large load gains for TEL (35%-62%) for the same target blocking probability. The higher node count and mesh degree of TEL combined by its link distances making signal overlap feasible are the most relevant network features behind such good performance. Note that traffic profile is also important; thus, the higher is the amount of demands destination sharing (which increases from TP-1 to TP-3), the higher is the amount of possible combinations of pair of demands to overlap and hence, the higher are the potential benefits of the technique.

A detailed analysis of the amount of connections using each of the modulation formats as well as the average number of used spectrum slices per demand is presented in Fig. 5. As can be observed, in the absence of signal overlapping more than 95% of demands are routed using 16-QAM. Working signal overlap scheme slightly increases the amount of QPSK connections, which is related with the small network performance gain observed in Fig. 4. The largest difference with respect to these two schemes is clearly observable for working and backup overlap scheme. Indeed, 45% and 70% of demands for DT and TEL respectively, are routed using QPSK, which is proportionally related to the amount of performed signal overlap. In addition, average used spectrum resources per demand sharply decreases for TEL, which is

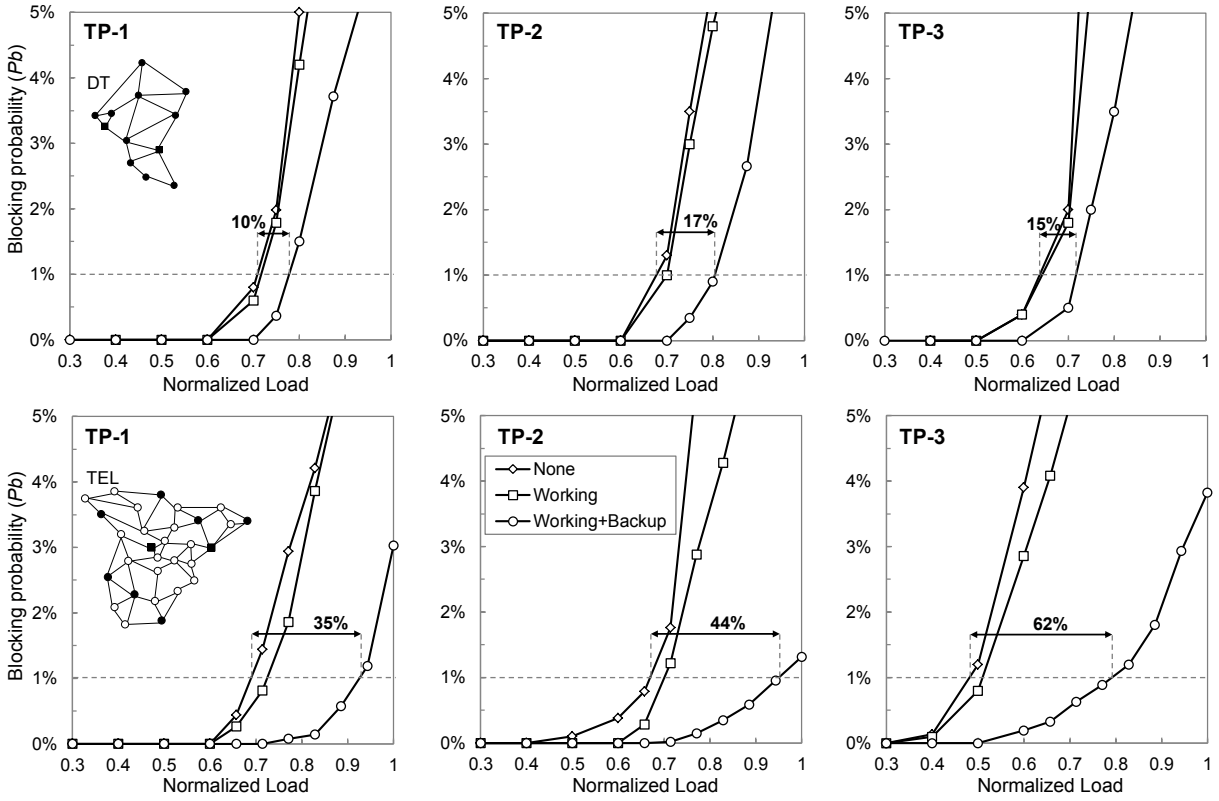


Fig. 4. Blocking probability vs normalized load

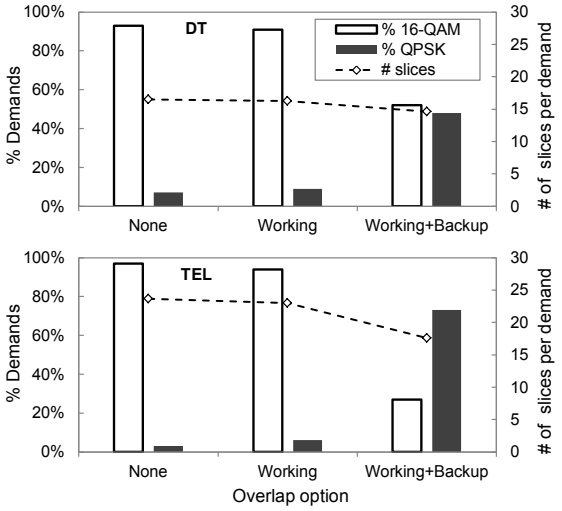


Fig. 5. MF and spectrum usage analysis for TP-2

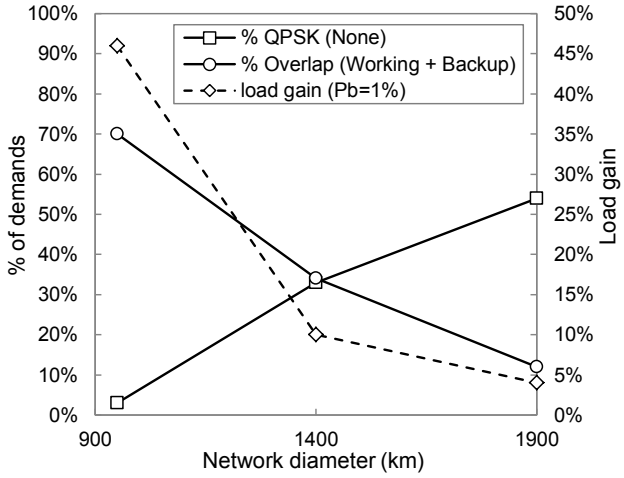


Fig. 6. Network diameter analysis for TEL and TP-2

another indicator of an advantageous signal overlap.

Finally, the relation between demands path length and signal overlap benefits is analyzed in Fig. 6. To this aim, distances of TEL topology links were proportionally increased in order to obtain two additional topologies with 1400 km and 1900 km of diameter, respectively. It is worth noting that increasing network length entails increasing the amount of connections using QPSK in the absence of overlap. This could be *a priori* interpreted as beneficial for signal overlap since less demands need to be extended from 16-QAM to QPSK with the expense of those additional spectrum resources to subtract to signal overlap spectrum savings.

However, since signal overlap technique has a maximum distance limit, increasing network length reduces the possibilities to apply it and consequently, diminishes network performance gain, until reaching negligible levels when diameter doubles the original one from TEL. Hence, we can

conclude that overlap both working and backup paths returns always the best performance, which is maximized when network characteristics (size, mesh degree, and diameter) and traffic profile allow exploiting overlap for a wide range of demands.

## VI. Concluding Remarks

In this study, the recently introduced signal overlap technique is proposed in the context of optical dedicated path protection (1+1). In particular, signal overlap is applied to take advantage of the surplus of QoT and spectrum resources available along the less impaired working path. The signal overlap technique, enabling uncorrelated optical signals to be superimposed along the same spectrum resources, enables up to 800 km (on 3-dB margin from theoretical bounds) to be covered by overlapped signals. A discussion on its implementation complexity is also reported, showing that the increased processing at the receiver is less relevant than expected and similar to an equalization process.

Two signal overlap schemes are introduced. The *working signal overlap* scheme applies the technique on working signals only, whereas the *working and backup signal overlap* scheme enables signal overlap on both working and backup paths. In order to evaluate the performance of both schemes, the PROSPECT problem is presented. An ILP formulation and an efficient heuristic are then presented to efficiently solve it.

The performance of the proposed schemes is then accurately evaluated under various topologies and traffic profiles. In the considered simulative scenarios where only dedicated protection requests are intentionally assumed, results have shown that applying signal overlap on working paths only (i.e., *working signal overlap* scheme) does not provide relevant benefits. On the other hand, the more efficient *working and backup signal overlap* can provide remarkable improvements on the accepted load with respect to traditional solutions exploiting dedicated frequency slots with no overlap. Moreover, significant benefits can be achieved for topologies presenting higher node count and mesh degree, network diameters well below thousand kilometers and traffic profiles with large amount of demands sharing destination nodes (e.g., hub-and-spoke scenarios).

## Acknowledgment

This work was partially supported by the EC through the METRO-HAUL project (grant agreement 761727) and from the Spanish MINECO SYNERGY project (TEC2014-59995-R).

## References

[1] F. Cugini, N. Sambo, M. Foggi, T. Ruiz, L. Velasco, and P. Castoldi, “Signal overlap for effcient 1+1 protection in elastic optical networks (eons),” in *OFC, Conf.*, 2017.

[2] M. Jinno et al., “Distance-adaptive spectrum resource allocation in spectrum-sliced elastic optical path network,” *Comm. Magazine*, 2010.

[3] D. Ly-Gagnon, S. Tsukamoto, K. Katoh, and K. Kikuchi, “Coherent detection of optical quadrature phase-shift keying signals with carrier phase estimation,” *J. Lightwave Tech.*, vol. 24, no. 1, pp. 12–21, 2006.

[4] F. Cugini, G. Meloni, F. Paolucci, N. Sambo, M. Secondini, L. Gerardi, L. Potì, and P. Castoldi, “Demonstration of flexible optical network based on path computation element,” *J. Lightwave Tech.*, vol. 30, no. 5, pp. 727–733, 2012.

[5] I. B. Djordjevic, M. Cvijetic, L. Xu, and T. Wang, “Using LDPCcoded modulation and coherent detection for ultra highspeed optical transmission,” *J. Lightwave Tech.*, vol. 25, no. 11, pp. 3619–3625, 2007.

[6] N. Sambo, G. Meloni, F. Paolucci, F. Cugini, M. Secondini, F. Fresi, L. Poti, and P. Castoldi, “Programmable transponder, code and differentiated filter configuration in elastic optical networks,” *J. Lightwave Tech.*, vol. 32, no. 11, pp. 2079–2086, June 2014.

[7] ITU-T, “Spectral grids for WDM application: DWDM frequency grid,” *G. 694.1*, 2012.

[8] Y. Li, D. King, F. Zhang, and A. Farrel, “Generalized labels for the flexigrid in lambda-switch-capable (LSC) label switching routers,” *draft-ietfccamp-flexigrid-lambda-label-04*, 2015.

[9] T. Foggi and F. Cugini, “Signal overlap for elastic optical networks,” *J. Lightwave Tech.*, 2015.

[10] G. Meloni, T. Foggi, F. Paolucci, F. Fresi, F. Cugini, P. Castoldi, G. Colavolpe, and L. Potí, “First demonstration of optical signal overlap,” in *Photonics in Switching (PS)*, Conf., 2014, pp. NM4D–4.

[11] Y. Saito et al., “Non-orthogonal multiple access (NOMA) for cellular future radio access,” *VTC*, June 2013.

[12] A. Barbieri, D. Fertonani, and G. Colavolpe, “Time-frequency packing for linear modulations: spectral efficiency and practical detection schemes,” *IEEE Trans. Commun.*, vol. 57, pp. 2951–2959, Oct. 2009.

[13] T. Foggi, G. Colavolpe, A. Bononi, and P. Serena, “Spectral efficiency optimization in flexi-grid long-haul optical systems,” *Journal of Lightwave Technology*, vol. 33, no. 13, pp. 2735–2742, 2015.

[14] R. Goscien et al., “Protection in elastic optical networks,” *IEEE Network*, vol. 29, no. 6, pp. 88–96, Nov 2015.

[15] M. Ruiz and L. Velasco, "Serving Multicast Requests on Single Layer and Multilayer Flexgrid Networks," IEEE/OSA Journal of Optical Communications and Networking (JOCN), 7, 146-155, 2015.

[16] D. M. Arnold, H.-A. Loeliger, P. O. Vontobel, A. Kav˘ci´c, and W. Zeng, “Simulation-based computation of information rates for channels with memory,” *IEEE Trans. Inform. Theory*, vol. 52, no. 8, pp. 3498–3508, Aug. 2006.

[17] G. Colavolpe and T. Foggi, “Time-frequency packing for high capacity coherent optical links,” IEEE Trans. Commun., vol. 62, no. 8, pp. 2986-2995, Aug. 2014.

[18] “Finisar Waveshaper,” in *https://www.finisar.com/optical-instrumentation/ waveshaper-16000s-multiport-optical-processor.*

[19] E. M. Ip and J. M. Kahn, “Fiber Impairment Compensation Using Coherent Detection and Digital Signal Processing”, Journal of Lightwave Technology (JLT), vol. 28, pp. 502-519, Feb 2010.

[20] H. Wymeersch and H. Steendam and M. Moeneclaey, “Log-domain decoding of LDPC codes over GF(q)”, IEEE International Conference on Communications, June 2004

[21] L. Velasco, A. P. Vela, F. Morales, and M. Ruiz, "Designing, Operating and Re-Optimizing Elastic Optical Networks," (Invited Tutorial) IEEE/OSA Journal of Lightwave Technology (JLT), 2017.

[22] L. Velasco, A. Castro, M. Ruiz, and G. Junyent, "Solving Routing and Spectrum Allocation Related Optimization Problems: from Off-Line to In-Operation Flexgrid Network Planning," (Invited Tutorial) IEEE/OSA Journal of Lightwave Technology (JLT), vol. 32, pp. 2780-2795, 2014.